Model Based Decoupling Control for Waste Incineration Plants

Martin Kozek[†] and Andreas Voigt[‡]
[†]Institute of Mechanics and Mechatronics, Vienna University of Technology, Vienna, Austria
Email: kozek@impa.tuwien.ac.at
[‡]VOIGT+WIPP Engineers GmbH, Vienna, Austria
Email: voigt@at.vo-wi.eu

Abstract— **A simple yet effective approach for a decoupling control of a waste incineration plant with fluidized bed is presented. The main problems for designing a decoupling controller are the nonlinear inner dynamics of the process, large time-delays, and unknown model parameters. The proposed control scheme utilizes the inversion of simple balance equations with a minimum of parameters and compact nonlinear characteristics. The main advantage of this concept is the simple incorporation of all relevant inputs and outputs of the plant into the decoupling equations. This ensures robust performance even in the presence of nonmeasurable disturbances and simple retrofitting. The proposed control scheme has been implemented in a 38 MW domestic waste incineration plant and the performance is demonstrated by measurements.**

Keywords—**decoupling control, waste incineration, model based decoupling.**

I. INTRODUCTION

Fluidized bed incinerators represent state of the art technology for waste combustion and low grade fuels. Additionally, sewage sludge can be incinerated to form stabilized ash and to reduce the volume for depositing. The main advantages of this process are high fuel flexibility in a large calorific value range, optimal combustion can be adjusted through combustion air and recirculation gas, high burnout (typical residues level in bed ash is $\leq 0.1\%$), low flue gas emissions, and limited mechanical processing of both fuel and ashes.

However, waste incineration plants are characterized by strong couplings between manipulated variables and control variables, nonlinearities with respect to operating points, time delays, largely differing time constants, and uncertainties in model parameters [1], [2], [3]. The control schemes of fluidized bed plants are currently mainly conventional, consisting of proportional-integral derivative (PID)-type controllers in separate control loops. In order to compensate effects of the nonlinear and strongly coupled process, static decoupling together with gain scheduling has been employed [4]. Nevertheless, the process performance shows strong variations and interventions of the plant operator are frequent.

In this paper a model inversion based approach is proposed, where the familiar problem of an imperfect model match is overcome by incorporating all relevant measured inputs and outputs of the process into the inversion. This multi-variable feedback concept for decoupling is shown to be robust in the presence of disturbances and with respect to model errors. Moreover, the proposed control scheme requires a minimum of analytical and experimental modeling. The computational effort is small, and the proposed concept can be directly implemented in any modern distributed control system (DCS).

Standard methods for decoupling can be found in [5], [6], in modified form in [7]. These concepts use only the manipulated variables for decoupling while the proposed decoupling scheme uses all relevant inputs and outputs of the process. Exact linearization [5], [8] requires a complete nonlinear state-space model of the system, and the resulting pseudo-linear system is generally still coupled. More complex methods are necessary to obtain decoupled pseudo-linear subsystems as demonstrated in [3]. A different approach is given by model reference adaptive control (MRAC), which has been proposed as an efficient and globally stable control scheme [1], [2]. However, this algorithm is mathematically complex, cannot be fitted into an existing control scheme, and the treatment is limited to a 2-input 2-output system without power generation.

Decoupling control schemes can also be found for power plant applications, where either adaptive algorithms using fuzzy logic [9], a hybrid classical/fuzzy approach [10], or recurrent artificial neural nets [11] have been proposed or implemented. All of these methods rely on either expert knowledge of plant operation or extensive training data.

The remainder of this paper is structured as follows: In Section II the plant is described and the variables are defined. The control concept is outlined in Section III, and in Section IV the respective model equations and control laws are developed. In Section V simulation results are presented, and in Section VI the excellent performance of the proposed scheme is demonstrated by an industrial implementation.

II. FLUIDIZED BED WASTE INCINERATION PLANT

Fluidized bed furnaces are used for waste incineration due to their applicability for the combustion of solid waste as well as sewage sludge. Many facilities serve a threefold purpose:

1) Environmentally correct and efficient disposal of waste.
2) Steam generation for conversion to electric energy.
3) Utilization of waste heat for district-heating.

978-1-4244-1718-6/08/$25.00 ©2008 IEEE

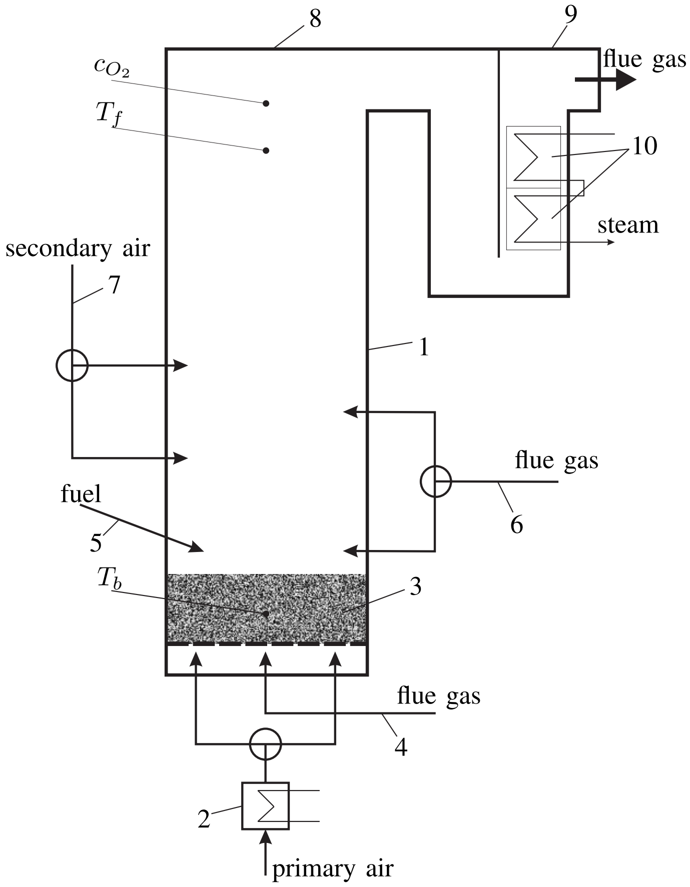

Fig. 1. Plant scheme for a fluidized bed furnace

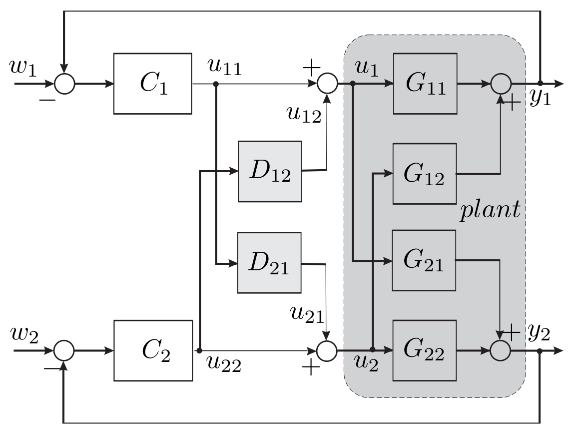

Fig. 2. Conventional decoupling for a 2-input / 2-output system

A schematic drawing of a typical plant is depicted in Fig. 1. Primary air is fed through an air heater (2) into the fluidized bed (3) from the bottom of the furnace (1). A portion of the flue gas is recycled and also fed into the fluidized bed (4) together with the primary air. Inside the fluidized bed the bed temperature T_b is measured. Fuel (5) is fed into the fluidized bed. Above the fluidized bed secondary air (7) as well as recycled flue gas (6) are blown into the furnace at different levels. At the top part of the furnace (8) the furnace temperature T_f and the concentration of oxygen c_{O_2} are measured. The hot flue gas is led into a heat recovery boiler (HRB) (9), where heat is transferred to a heat exchanger (10). Finally, the flue gas is filtered, cleaned, and part of it is recycled.

One of the main technological challenges of this process is the fluidization of the bed. The bed consists of inert media (silicate sand), solid waste, possibly sludge and additional fuel. As described above, fluidization is achieved by blowing gas into the bed from below. Controlled variables y_i of the fluidized bed furnace (including HRB) are:

1) y_1: O_2-concentration at the top c_{O_2} $[\%_{vol}]$ (and/or after the HRB)
2) y_2: total power of combustion P_Σ $[kW]$ or live steam produced $\dot{m}_s\left[\frac{t}{h}\right]$
3) y_3: furnace temperature T_f $[°C]$ at the top
4) y_4: bed temperature T_b $[°C]$

Manipulated variables u_i of the furnace are:

1) u_1: Volume flow of secondary air $\dot{V}_s$ $\left[\frac{m^3}{s}\right]$
2) u_2: Volume flow of recycled flue gas *above* bed $\dot{V}_r$ $\left[\frac{m^3}{s}\right]$
3) u_3: Volume flow of primary air $\dot{V}_p$ $\left[\frac{m^3}{s}\right]$
4) u_4: Volume flow of recycled flue gas *below* bed $\dot{V}_r^*$ $\left[\frac{m^3}{s}\right]$
5) u_5: Fuel mass flow $\dot{m}_f$ $\left[\frac{kg}{s}\right]$

Additionally measured output variables are:

1) y_5: temperature of recirculation gas T_r $[°C]$
2) y_6: O_2-concentration in recirculation gas $c_{O_2,r}$ $[\%_{vol}]$

III. Control Concept

The basic concept is a decoupling network within a multi-variable control scheme, and the resulting control scheme consists of pseudo-linear, independent, and parallel control loops. In the following sections first conventional decoupling is described and then the proposed model based approach is outlined.

A. Conventional decoupling

In Fig. 2 a conventional decoupling scheme for a linear 2×2 process is shown. Two inputs u_1 and u_2 and two outputs y_1 and y_2 with reference variables w_1 and w_2 are considered. The outputs of the plant are defined by:

$$\begin{aligned} Y_1(s) &= G_{11}(s)U_1(s) + G_{12}(s)U_2(s) \\ Y_2(s) &= G_{21}(s)U_1(s) + G_{22}(s)U_2(s). \end{aligned} \tag{1}$$

A decoupling transfer function D_{21} is designed such that the output U_{21} satisfies

$$G_{21}(s)U_{11}(s) + G_{22}(s)U_{21}(s) = 0. \tag{2}$$

By substituting $U_{21} = D_{21}U_{11}$ into (2)

$$(G_{21}(s) + G_{22}(s)D_{21}(s))U_{11}(s) = 0 \tag{3}$$

follows, and observing that in general $U_{11}(s) \neq 0$ the ideal decoupler's transfer functions are given by

$$\begin{aligned} D_{21}(s) &= -\frac{G_{21}(s)}{G_{22}(s)} \\ D_{12}(s) &= -\frac{G_{12}(s)}{G_{11}(s)}. \end{aligned} \tag{4}$$

Ideal decouplers are not always physically realizable or sensitive to modeling errors; standard procedures to avoid or minimize these problems are (see [5], [6])

- Partial decoupling: only a subset of decouplers is used.
- Static decoupling: only the static gains of the decoupler's transfer functions are implemented.

Obviously, these methods will reduce the control performance, and in the presence of strong nonlinearities and non-measurable disturbances the performance of the conventional decoupling control will be poor.

B. Model Based Decoupling

In general, every MIMO-plant with m scalar control loops can be modeled by a state-space representation with m inputs u_j, n state variables x_i, and a parameter vector $\boldsymbol{\theta}$. In the special case where all states can be directly measured ($y_i = x_i$) a set of n first-order state equations

$$\frac{dy_i}{dt} = f_i(\boldsymbol{y}, \boldsymbol{u}, \boldsymbol{\theta}), \;\; i = 1, \ldots, n \tag{5}$$

together with a set of n algebraic output equations

$$y_i = g_i(\boldsymbol{y}, \boldsymbol{u}, \boldsymbol{\theta}), \tag{6}$$

constitute the complete plant model, and $\boldsymbol{u}$ and $\boldsymbol{y}$ denote input and output vectors, respectively. The nonlinear functions f_i and g_i are typically derived from non-stationary and stationary balances of the plant's variables.

In both sets of equations (5) and (6) the dependence of each plant output y_i on all other plant outputs and inputs u_j is explicitly stated. Now a subset of $m \leq n$ outputs $\tilde{\boldsymbol{y}} \subset \boldsymbol{y}$ is defined, where each $\tilde{y}_j$ is the controlled variable of one of the m scalar control loops (see Fig. 3). In the right hand sides of (5) and (6) the influence of all control inputs to a specific controlled variable $\tilde{y}_j$ is uniquely defined. Rearranging for the respective control variable u_j of that specific control loop yields an equation

$$\tilde{y}_j = \tilde{f}_j(\boldsymbol{y}, \boldsymbol{u}, \boldsymbol{\theta}). \;\; j = 1, \ldots, m \tag{7}$$

Note that the nonlinear function $\tilde{f}_j$ may be composed from a dynamic relation (5) or it may result from a static relation (6). In any case, a necessary condition for the construction of a decoupling structure is that:

Necessary condition I for decoupling: The expression $\tilde{f}_j$ for each controlled variable $\tilde{y}_j$

$$\tilde{y}_j = \tilde{f}_j(\boldsymbol{y}, \boldsymbol{u}, \boldsymbol{\theta}), \tag{8}$$

must explicitly contain the corresponding manipulated variable u_j such, that the manipulated variable u_j is either multiplied

$$\tilde{y}_j = \bar{f}_j(\boldsymbol{y}, \boldsymbol{u}, \boldsymbol{\theta})\, u_j \tag{9}$$

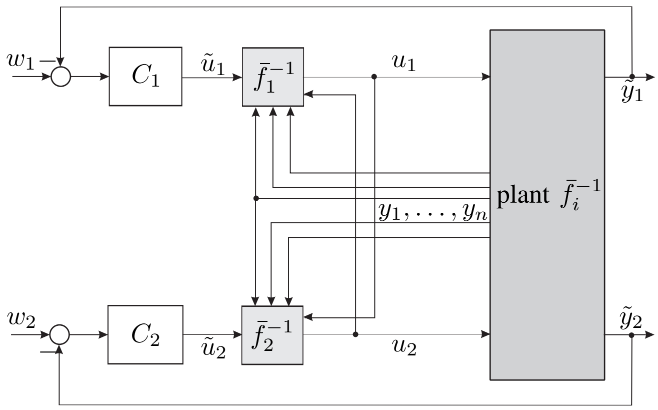

Fig. 3. Nonlinear decoupling with model based inversion.

or

Necessary and sufficient condition Ia for decoupling: The manipulated variable u_j is additively coupled

$$\tilde{y}_j = \bar{f}_j(\boldsymbol{y}, \boldsymbol{u}, \boldsymbol{\theta}) + \alpha u_j. \tag{10}$$

to the remaining nonlinear expression $\bar{f}_j$ (α being a constant factor).

In the case of an additive manipulated variable (10) the control law can be formulated as

$$u_j = \frac{1}{\alpha}\left[\tilde{y}_j - \bar{f}_j(\boldsymbol{y}, \boldsymbol{u}, \boldsymbol{\theta})\right], \tag{11}$$

where no inversion of the nonlinear expression $\bar{f}_j$ is necessary. On the other hand, the structure of (9) requires another necessary condition to be met:

Necessary condition II for decoupling: The expression $\bar{f}_j$ in (9) must be invertible such, that

$$u_j = \bar{f}_j^{-1}(\boldsymbol{y}, \boldsymbol{u}, \boldsymbol{\theta})\tilde{y}_j, \tag{12}$$

exists. The computation of $\bar{f}_j^{-1}$ requires $\bar{f}_j$ to be invertible with respect to u_j. This is not a strong restriction, especially for basic balance equations and stoichiometric relations as often emerging while modeling incineration plants.

In this case the necessary condition II is already the control law defining the manipulated variable u_j. Both control laws (11) and (12) can be directly implemented according to Fig. 3, if the substitution

$$\tilde{y}_j = \tilde{u}_j \tag{13}$$

is made. Then the governing relations for the control loop with index 1 in Fig. 3 are given by:

$$\begin{aligned} \tilde{u}_1 &= C_1(q^{-1})\,(w_1 - \tilde{y}_1) & (14)\\ u_1 &= \bar{f}_1^{-1}(\boldsymbol{y}, \boldsymbol{u}, \boldsymbol{\theta})\tilde{u}_1 & (15)\\ u_1 &= \bar{f}_{1,plant}^{-1}(\boldsymbol{y}, \boldsymbol{u}, \boldsymbol{\theta})\tilde{y}_1 & (16) \end{aligned}$$

The manipulated variable can therefore be expressed as

$$\begin{aligned} u_1 &= \bar{f}_1^{-1}(\boldsymbol{y}, \boldsymbol{u}, \boldsymbol{\theta})\tilde{u}_1 \\ &= \bar{f}_1^{-1}(\boldsymbol{y}, \boldsymbol{u}, \boldsymbol{\theta})C_1(q^{-1})\,(w_1 - \tilde{y}_1)\,, \end{aligned} \tag{17}$$

and (16) with (17) yields

$$\bar{f}_{1,\,plant}^{-1}(\boldsymbol{y},\boldsymbol{u},\boldsymbol{\theta})\tilde{y}_1 = \bar{f}_1^{-1}(\boldsymbol{y},\boldsymbol{u},\boldsymbol{\theta})C_1(q^{-1})\,(w_1 - \tilde{y}_1)\,. \tag{18}$$

Only if the model $\bar{f}_1^{-1}$ is identical to the plant's inverted nonlinearity $\bar{f}_{1,\,plant}^{-1}$ a complete cancelation of the nonlinearities becomes possible

$$\begin{aligned}\tilde{y}_1 &= C_1(q^{-1})\,(w_1 - \tilde{y}_1)\\ \tilde{y}_1 &= \frac{C_1(q^{-1})}{1 + C_1(q^{-1})}w_1 = G_{w1}(q^{-1})w_1,\end{aligned} \tag{19}$$

which is the standard closed-loop expression where the open loop transfer function is given by $C_1(q^{-1})$. Note that (19) states that the plant output $\tilde{y}_1$ will follow the reference w_1 with arbitrary dynamics defined by $G_{w1}(q^{-1})$ and zero position error, if the static gain of $G_{w1}(q^{-1})$ is equal to one.

The expression $\bar{f}_j$ in (10) can be a differential or algebraic equation, respectively, depending on whether an equation of type (5) or (6) was chosen when defining $\tilde{f}_j$ in (7).

In contrast to conventional decoupling, the decoupling expressions $\bar{f}_1^{-1}$ and $\bar{f}_2^{-1}$, respectively, are

- in general nonlinear,
- utilize a number of output variables of the plant,
- based on very general model equations of the plant.

Observe that each decoupler $\bar{f}_i^{-1}$ in Fig. 3 already represents a feedback loop, where all measured outputs y_i are used to compute the actual feedback u_j. If one or more inner variables of the plant change due to unmeasured disturbances a disturbance compensation is automatically performed by the decoupler according to (12).

IV. Plant Model and Controller Design

A. Plant Model

The combustion and power generation process is described by the controlled variables: 1) furnace temperature T_f 2) O_2-concentration at top of furnace c_{O_2} 3) bed temperature T_b and 4) live steam produced $\dot{m}_s$. In order to decouple the four main control loops the governing model equations for each loop are presented in the following.

1) Model for Oxygen Concentration: The main variable for oxygen control is the momentary rate of oxygen build-up $\dot{V}_{O_2}$ of the combustion. This variable can be computed from measured outputs by a balance of oxygen in the furnace

$$\dot{V}_{O_2} = \dot{V}_{O_2+} - \dot{V}_{O_2-}, \tag{20}$$

where (20) is given by

$$\dot{V}_{O_2} = \left(\dot{V}_s + \dot{V}_p\right) c_{O_2,\,air} + \left(\dot{V}_r + \dot{V}_r^*\right) c_{O_2,\,r} - \dot{V}_f\, c_{O_2}. \tag{21}$$

The variable $\dot{V}_f$ denotes the total flue gas at the top of the furnace. Note that the specific oxygen demand of the fuel defined as

$$\hat{k}_f = \frac{\dot{V}_{O_2}}{\dot{m}_f} \tag{22}$$

can be readily computed from measured outputs using (21).

2) Model for Furnace Temperature: The furnace temperature T_f can be described by an unsteady balance of the enthalpy flows into or from the furnace. The basic equation is given by

$$C_f \frac{dT_f}{dt} = \sum_i \Delta H_i = \Delta H_p + \Delta H_s + \Delta H_r + P_c, \tag{23}$$

where C_f is the absolute heat capacity of the furnace and the net enthalpy contributions from the individual gas flows (primary air, secondary air, and recirculated gas) are

$$\begin{aligned}\Delta H_p &= \dot{V}_p c_{p,\,air}\, \rho_{air}\,(T_p - T_f)\\ \Delta H_s &= \dot{V}_s c_{p,\,air}\, \rho_{air}\,(T_s - T_f)\\ \Delta H_r &= \dot{V}_r c_{p,\,r}\, \rho_r\,(T_r - T_f)\\ P_c &= \sum_j H_{n,\,j}\, \dot{m}_{f,\,j}\end{aligned} \tag{24}$$

and P_c denotes the sum of power released by the combustion of different fuel components of a net calorific value $H_{n,\,j}$. The variables $c_{p,\,i}$ in (24) denote the specific heat of the individual gases, and the ρ_i denote their respective densities.

3) Model for Bed Temperature: The bed temperature is described by two relations: The dependence of the bed temperature on the air ratio and the respective oxygen balance. The oxygen balance equation for the fluidized bed is given by

$$V_b \frac{dc_{O_2}}{dt} = \sum_i \dot{m}_{O_2,\,i} = \dot{m}_{O_2,\,p} + \dot{m}_{O_2,\,r} + \dot{m}_{O_2,\,c}, \tag{25}$$

where V_b is the volume of the fluidized bed and the individual right-hand expressions (oxygen mass flows) are

$$\begin{aligned}\dot{m}_{O_2,\,p} &= \dot{V}_p c_{O_2,\,p}\, \rho_{air}\\ \dot{m}_{O_2,\,r} &= \dot{V}_r^* c_{O_2,\,r}\, \rho_r\\ \dot{m}_{O_2,\,c} &= \lambda \sum_j k_{f,\,j}\, \dot{m}_{f,\,j}.\end{aligned} \tag{26}$$

A nonlinear static model of the bed temperature

$$T_b = f(\lambda, \dot{V}_{fluid}), \tag{27}$$

was identified from measured data. The dependence from the air ratio becomes one-dimensional if the total gas flow for fluidization $\dot{V}_{fluid}$ is kept constant:

$$\dot{V}_p + \dot{V}_r^* = \dot{V}_{fluid} = const. \tag{28}$$

4) Model for Live Steam Production: Under the assumption of a stoichiometric combustion the amount of live steam produced is coupled to the fuel consumption of the combustion. The influence of other manipulated variables like T_b, T_k, or $\dot{V}_r$ will be comparably insignificant. Since the HRB and therefore the mass flow of live steam is situated at the very end of the considered plant an analytical model will be complex and contain many unknown parameters. A linear transfer function model G_{fs}

$$\dot{m}_s = G_{fs}(q^{-1})\dot{m}_f \tag{29}$$

therefore has a considerable time-delay. However, during stoichiometric combustion the fuel mass flow $\dot{m}_f$ requires an appropriate total oxygen flow $\dot{V}_{\Sigma,O_2}$:

$$\dot{V}_{\Sigma,O_2} = \bar{k}_f \dot{m}_f \tag{30}$$

Here, $\bar{k}_f$ is the mean oxygen demand of the fuel which is known from continual laboratory measurements. The variable $\dot{V}_{\Sigma,O_2}$ is given by

$$\begin{aligned} \dot{V}_{\Sigma,O_2} &= \left(c_{O_2,air} - c_{O_2}\right)\left(\dot{V}_p + \dot{V}_s\right) \\ &+ \left(c_{O_2,r} - c_{O_2}\right)\dot{V}_r - V_f \frac{dc_{O_2}}{dt}. \end{aligned} \tag{31}$$

V_f is the total volume of the furnace, and the expression $V_f \frac{dc_{O_2}}{dt}$ constitutes an oxygen drain due to chemical consumption in the combustion.

B. Controller Design

1) Control Law for Oxygen Control: The secondary air flow for perfect combustion can be calculated from the model (21) together with (22). The secondary air flow is defined as

$$\dot{V}_s = \frac{\dot{m}_f \cdot \hat{k}_f + \dot{V}_f\, c_{O_2} - \dot{V}_p c_{O_2,air} - \left(\dot{V}_r + \dot{V}_r^*\right) c_{O_2,r}}{c_{O_2,air}} \tag{32}$$

2) Control Law for Furnace Temperature Control: The furnace temperature T_k is controlled by the flow of the recirculated flue gas above the bed. Rearranging (23) gives

$$\Delta H_r = C_k \frac{dT_k}{dt} - \Delta H_p - \Delta H_s - P_c, \tag{33}$$

and inserting the relations (24) and solving for $\dot{V}_r$ yields

$$\dot{V}_r = \frac{C_k \frac{dT_k}{dt} - \Delta H_p - \Delta H_s - P_c}{c_{p,r}\, \rho_r \left(T_r - T_f\right)}. \tag{34}$$

3) Control Law for Bed Temperature Control: Using (28) the recirculation gas flow into the bed is given by

$$\dot{V}_r^* = \dot{V}_{fluid} - \dot{V}_p. \tag{35}$$

Inserting (35) in (25) and rearranging for $\dot{V}_p$ yields the control law

$$\dot{V}_p = \frac{V_b \frac{dc_{O_2}}{dt} - V_{fluid} c_{O_2,r}\, \rho_r - \lambda \sum_j k_{f,j}\, \dot{m}_{f,j}}{c_{O_2,p}\, \rho_{air} - c_{O_2,r}\, \rho_r}. \tag{36}$$

In (36) the air ratio λ can be computed from the desired bed temperature T_b using the inverse of (27) for a given $\dot{V}_{fluid}$:

$$\lambda = f^{-1}(T_b) \tag{37}$$

4) Control Law for Live Steam Control: The fuel feeding rate can be computed from the inversion of the model (29) as $\dot{m}_f = G_{fs}^{-1}(q^{-1})\dot{m}_s$ only if $G_{fs}^{-1}(q^{-1})$ is realizable. Since this is not the case, the necessary fuel rate is computed from (30) and (31) as

$$\begin{aligned} \dot{m}_f &= \frac{1}{\bar{k}_f}\Big[\left(c_{O_2,air} - c_{O_2}\right)\left(\dot{V}_p + \dot{V}_s\right) \\ &+ \left(c_{O_2,r} - c_{O_2}\right)\dot{V}_r - V_f \frac{dc_{O_2}}{dt}\Big]. \end{aligned} \tag{38}$$

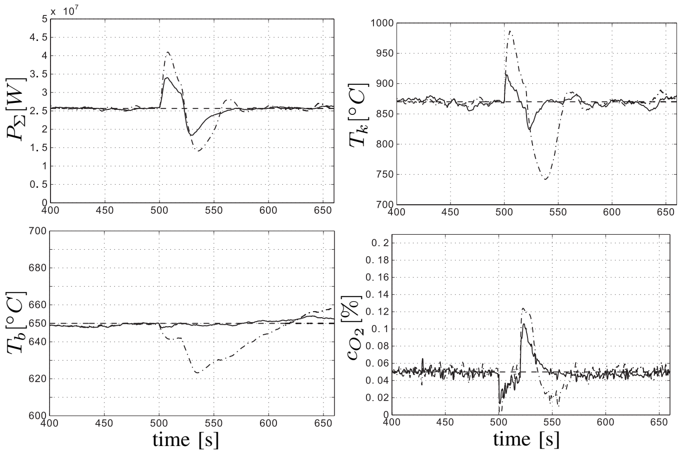

Fig. 4. Simulation results. Top left: thermal power, top right: furnace temperature, bottom left: bed temperature, bottom right: oxygen concentration at top of furnace. Solid line - new control, dash-dotted line - original control, dashed line - set-point.

V. Simulation Study

A numeric simulation study was performed in order to assess the possible improvements of the proposed control scheme. The simulation consists of detailed non-stationary sub-models of all plant sections. All actuating elements are modeled with saturations and limitations in actuation rate. Stochastic models have been used for the calorific value $\bar{H}_f$ (average 9.5 MJ/kg_{fuel}, standard deviation 0.63 MJ/kg_{fuel}) and the mean oxygen demand of the fuel $\bar{k}_f$ (average 14.8 kg_{air}/kg_{fuel}, standard deviation 1 kg_{air}/kg_{fuel}). The simulation model was validated using measured data from the plant. Due to sensor noise the non stationary expressions $\frac{dy_i}{dt}$ in the control laws (34), (36), and (38) were omitted.

A. Simulation Results

The simulation demonstrates the effect of a sudden increase in fuel feed of 50% at t=500s for a duration of 20s. Original control and the proposed decoupling scheme are compared. The parameters of the linear controller transfer functions C_i the are identical in both cases.

In Fig. 4 top left plot the deviation of the thermal power of the HRB is shown. A reduction of approximately 50% is visible. In the top right plot the furnace temperature is shown. The reduction in amplitude is around 70% with a much reduced error effect. The bottom left plot demonstrates an almost perfect decoupling for the bed temperature. Any remaining coupling effects are masked by the stochastic fluctuations. In the bottom right plot the variation in oxygen concentration is shown. Strong reductions and a much earlier compensation can be seen.

Although most outputs still show coupling effects due to imperfect implementation of the model, all amplitudes and disturbance durations are strongly reduced. Moreover, the performance of the proposed decoupling is equally good over the whole operating region.

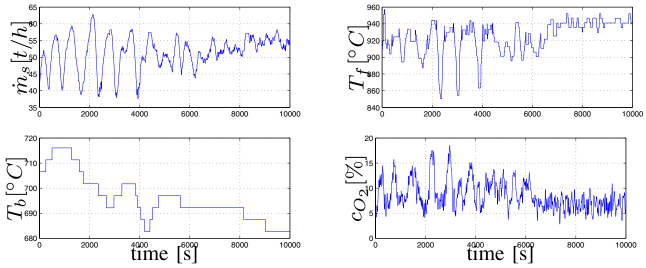

Fig. 5. Application results. Top left: live steam, top right: furnace temperature, bottom left: bed temperature, bottom right: oxygen concentration at top of furnace. The decoupling control is activated at t=6000 s.

TABLE I

INCREASE IN ABSOLUTE PLANT CAPACITY

variable	conventional	decoupling
waste capacity	max. 15 t/h	max. 17 t/h
steam production	45.6t/h	54.0 t/h

VI. INDUSTRIAL APPLICATION

The control scheme was implemented in a municipal waste incineration plant. Preprocessed domestic waste and sometimes additionally sewage sludge is incinerated. The plant has a maximum waste capacity of 12.5 t/h, a maximum wet sewage sludge capacity of 15.3 t/h (36% dry substance), a furnace capacity of 38.2 MW, and a maximum steam production of 45.6 t/h (at 54 bar and 354° C).

The decoupling control scheme was implemented on the existing DCS without the necessity for hardware or software extensions. For each individual control loop a fall-back possibility to the original control structure and parameters was programmed.

Some important data for the waste incineration plant are listed in table I. The absolute values of waste capacity and steam production have been significantly increased while the furnace temperature has been reduced simultaneously. The furnace temperature is a key variable for the service life expectancy of both furnace and HRB. In Fig. 5 results for the controlled variables are shown. At t=6000 s the new control is activated and after a short transient all variables show a significantly reduced variance. In table II the standard deviations of the controlled variables before and after implementation under stationary operation (full capacity) are shown. The reduction in variation is most important since it enables a plant operation closer to technological and legal limits. The reduction in variance of the controlled variables has different effects on the manipulated variables: Some of them also exhibit smaller activity (e.g. $\dot{V}_r$) while others show a significant increase both in amplitude and bandwidth (e.g. $\dot{m}_f$ and $\dot{V}_p$). Although not shown here, the control scheme is also performing excellent in part-load operating conditions.

TABLE II

STANDARD DEVIATIONS OF CONTROLLED VARIABLES

variable	σ	σ_{new}	unit
$\dot{m}_s$	5.55	2.17	t/h
c_{O_2}	2.86	1.38	%vol
T_B	8.80	4.06	°C
T_f	18.3	5.79	°C

VII. CONCLUSION

A model based decoupling control for a fluidized bed waste incineration plant has been presented. The decoupling control of the MIMO-plant is based on explicit physical models, as well as black-box models from system identification. If the models are invertible, a perfect decoupling between the individual control loops becomes possible. The main advantage of the proposed control scheme is the incorporation of all available plant outputs for a perfect decoupling; even if a this is not realizable a robust and efficient decoupling can be achieved. Furthermore, due to the explicit incorporation of all relevant plant outputs each decoupler also acts as a disturbance compensator for external disturbances. The performance of the proposed control scheme is demonstrated by a numeric simulation and in a full scale implementation. The comparison between the original and the decoupling scheme shows a substantial increase in efficiency and a minimization of cross-couplings and disturbances. Due to the compact formulation of the overall control scheme the implementation in a DCS is straightforward, and retrofitting of existing plants becomes easily possible.

A drawback of the proposed concept is the partly heuristic choice of the balance equations, where expert knowledge is definitely of advantage. Global stability of the proposed concept is still not analytically proven, which will be a task for future research.

REFERENCES

[1] Y. Jia, H. Kokame, and J. Lunze, "Simultaneous adaptive decoupling and model matching control of a fluidized bed combustor for sewage sludge," *IEEE Transactions on Control Systems Technology*, vol. 11, no. 4, pp. 571–577, 2003.

[2] H.-X. Meng and Y.-M. Jia, "Improved robust adaptive control of a fluidized bed combustor for sewage sludge," *Acta Automatica Sinica*, vol. 31, no. 4, pp. 562–566, 2005.

[3] F.-H. Song and P. Li, "Fluidized bed control system based on inverse system method," *Journal of Coal Science and Engineering*, vol. 11, no. 1, pp. 59–62, 2005.

[4] A. Kaya and H. Sternberg, "Advanced control applications for fluidized bed boilers," in *Proceedings of the 1987 Industrial Power Conference*, vol. 2, Atlanta, GA, USA, 1987, pp. 35–42.

[5] B. Ogunnaike and W. Ray, *Process Dynamics, Modeling, and Control*, ser. Topics in Chemical Engineering. Oxford University Press, 1994.

[6] D. Seborg, T. Edgar, and D. Mellichamp, *Process Dynamics and Control*. John Wiley & Sons, 2004.

[7] H. Wade, "Inverted decoupling: A neglected technique," *Advances in instrumentation and control, Instrument Society of America*, vol. 51, no. 1, pp. 357–369, 1996.

[8] H. Khalil, *Nonlinear Systems*. Macmillan Publishing Company, 1992.

[9] S. Li, H. Liu, W.-J. Cai, Y.-C. Soh, and L.-H. Xie, "A new coordinated control strategy for boiler-turbine system of coal-fired power plant," *IEEE Transactions on Control Systems Technology*, vol. 13, no. 6, pp. 943–954, 2005.

[10] W. Wang, H.-X. Li, and J. Zhang, "Intelligence-based hybrid control for power plant boiler," *IEEE Transactions on Control Systems Technology*, vol. 10, no. 2, pp. 280–287, 2002.

[11] X.-Y. Yang, D.-P. Xu, X.-J. Han, and H.-N. Zhou, "Predictive functional control with modified elman neural network for reheated steam temperature," in *Proceedings of the 4th International Conference on Machine Learning and Cybernetics*. Guangzhou: IEEE, August 18-21 2002.